Available online at www.sciencedirect.com
SCIENCE DIRECT®
Biochimica et Biophysica Acta 1609 (2003) 203–210
BIOCHIMICA ET BIOPHYSICA ACTA
BBA
www.bba-direct.com

Beauvericin-induced channels in ventricular myocytes and liposomes

K. Kouri[a,*], M. Lemmens[b], R. Lemmens-Gruber[a]

[a] *Institute of Pharmacology and Toxicology, University of Vienna, Althanstr. 14, 1090 Vienna, Austria*
[b] *Department of Plant Production Biotechnology, Institute for Agrobiotechnology, Konrad Lorenzstr. 20, 3430 Tulln, Austria*

Received 7 October 2002; received in revised form 9 December 2002; accepted 10 December 2002

Abstract

The antibiotic Beauvericin (BEA) was previously shown to express ionophoric properties under simple experimental systems. Its channel-forming activity was examined in inside–out patches of ventricular myocytes and synthetic membranes with the patch clamp and fluorescence imaging techniques. Current transitions to several open state levels were evident after wash-in. The BEA channel is cation-selective. Conductance and kinetics are presented for K^+ and Na^+ substates and main states. The pore was blocked by La^{3+}. In myocytes, the $[K^+]_i$ was reduced, while $[Na^+]_i$ and $[Ca^{2+}]_i$ increased, leading to cytolysis. These results indicate that BEA forms cation-selective channels in lipid membranes, which can affect the ionic homeostasis.

Keywords: Cyclodepsipeptide; Ionophore; Patch clamp; *Fusarium*; Fura

1. Introduction

Beauvericin (BEA) is a cyclic hexadepsipeptide consisting of an alternating sequence of three D-α-hydroxy-isovaleryl and three *N*-methyl-L-phenylalanyl groups. It was originally isolated from *Beauveria bassiana* [1] and has been detected since then in various fungal species, including *Fusarium* spp., a common contaminant of cereals [2,3]. Diseases in animals and humans following consumption of contaminated food have been often connected to the presence of mycotoxins [4]. However, direct evidence for a possible role of BEA in mycotoxicoses does not exist.

BEA has antibiotic [1], insecticidal [5,6], apoptotic [7] and cholesterol acyltransferase inhibitory properties [8]. Studies of the effect of BEA on mammalian tissue are scarce. With regard to multicellular preparations, BEA's inhibitory effects on pre-contracted smooth muscle [9,10] and cardiac muscle [10] have been reported. Inhibition of the L-type Ca^{2+} current by BEA in the NG108-15 neuronal cell line has been described [11].

Earlier physicochemical studies have proposed BEA to be an ionophore [12–14] with an ionic selectivity of $K^+ > Na^+ > Ca^{2+}$ [13] or $Ca^{2+} > K^+ > Na^+$ [12]. The dimensions of the central cavity can be adapted to the radius of the complexed ion by increasing the bond angles of the oxygen atoms [15]. In addition, "sandwiching" of BEA molecules during cation complexation was predicted. In lipid membranes, sandwich complexes have been proposed to exist in a stoichiometry of antibiotic/cation equal to 2:1 or 3:2 [16].

Ionophoric properties of any substance can theoretically be explained by a carrier and/or a channel-forming mechanism. In this study, detailed findings of the channel-forming activity of BEA in ventricular myocytes and synthetic membranes are shown. Preliminary data have been presented in an abstract form [17].

2. Materials and methods

2.1. Electrophysiological experiments on ventricular myocytes

Electrical activity was studied on freshly isolated ventricular myocytes of guinea pigs. The heart was excised and cannulated to a Langendorff apparatus via the aorta. Cells were isolated by retrograde perfusion with a protease/collagenase containing modified Tyrode's solution [18].

* Corresponding author. Tel.: +43-1-4277-55301; fax: +43-1-4277-9553.
E-mail address: katerina.kouri@univie.ac.at (K. Kouri).

0005-2736/02/$ - see front matter © 2002 Elsevier Science B.V. All rights reserved.
doi:10.1016/S0005-2736(02)00689-2

Electrodes pulled of borosilicate capillaries had a tip resistance of 5–10 MΩ. Currents were recorded with the patch clamp technique in the inside–out mode [19]. The pipette and bathing solutions used were of the same composition and contained 140 mM potassium aspartate, 2 mM $CaCl_2$, 2 mM $MgCl_2$, 2 mM Na_2ATP, 10 mM HEPES, titrated to pH 7.4 with KOH. BEA was added in the bathing solution at concentrations up to 1 μM, unless stated otherwise. Adding ATP to the bathing solution prevented activation of the K_{ATP} channels. For measuring currents carried by other monovalent cations and assessing permeability of the channel for anions, potassium aspartate was replaced by equimolar concentrations of KCl, K_2SO_4, NaCl, Na_2SO_4 or LiCl. Calculation of reversal potentials (E_{rev}) was realized by successive substitution of the 140 mM KCl (or NaCl) bathing solution for 70 and 175 mM. Permeability ratios were calculated according to the modified GHK equation $P_K/P_{Na} = \exp^{(\Delta E_{rev} F/RT)}$ under bi-ionic conditions (140 mM potassium aspartate in the pipette solution and 140 mM sodium aspartate in the bathing solution). The solutions used for studying the permeation of Mg^{2+} or Ca^{2+} consisted of 110 mM $MgCl_2$, 2 mM $CaCl_2$, 10 mM HEPES or 110 mM $CaCl_2$, 2 mM $MgCl_2$, 10 mM HEPES, both titrated at pH 7.4 with $Ca(OH)_2$. All experiments were performed at room temperature (18–25 °C).

2.2. Incorporation of BEA in synthetic membranes

Freeze–thaw liposomes (FTL) were prepared as previously described [20]. The lipid membranes consisted of L-α-phosphatidyl-choline,-ethanolamine,-L-serine and cholesterol (5:5:2:2 w/w). FTLs were produced in the standard aqueous solution (SAS) containing 100 mM KCl, 1 mM $CaCl_2$ and 5 mM HEPES titrated to pH 7.5 with Tris. After freezing in liquid nitrogen, the FTLs were thawed at room temperature for 10–15 min and 2 μL of the FTL suspension was diluted in the bath containing the SAS. Dilution of the FTLs resulted in an increase in surface blebbing. Patch pipettes were made from borosilicate capillaries and were filled with the SAS. The initial resistance of the pipette was 15–20 MΩ. Pipettes were sealed on the outer membrane of the FTL and patches were excised by short exposure of the tip of the pipette to the air. BEA was added in the bath in a final concentration of 1 up to 10 μM.

Experiments were carried out with liposome-free patches. The potential values indicate the bath potential with respect to the pipette potential. Positive ions flowing out of the pipette were defined as an inward current. Unless stated otherwise, both pipette and bath were filled with the SAS. In order to determine the selectivity of the channel, the KCl concentration in the bath was raised to 500 mM. Blockers were always added to the bath solution. Control experiments with blank patches and with the Tween 80/MeOH (1:2 w/w) suspension in concentrations up to 10 times the final experimental concentrations in the bath were performed ($n = 32$ and 25, respectively). No channel-forming activity could be detected.

2.3. Single channel data analysis

Electrophysiological measurements were carried out with an Axopatch-1D patch clamp amplifier (Axon Instruments, CA). Currents were filtered at 5 kHz with a dual variable filter (VBF 8, Kemo Ltd., Beckenham, Kent, UK), digitized via an AD converter (TL-1 interface, Axon Instruments) and sampled at 2–10 kHz. In the case of ventricular myocytes, data acquisition and storage were executed directly to a PC with the pCLAMP 5 software (Axon Instruments). Single channel current data from FTLs were stored on a FM magnetic tape recorder. Single channel analysis was performed with the ASCD software (G. Droogmans, Leuven, Belgium).

Open and closed times were determined by setting the threshold to 50% of the unitary current amplitude. They were then fitted with exponential probability density functions by the maximum likelihood method. Data are expressed as mean ± S.E.

2.4. Fluorescence ratio imaging

Ventricular myocytes were loaded in modified Tyrode's solution with either 1 μM FURA 2AM, 0.5 μM of the fluorescent Na^+ indicator SBFI or the K^+ indicator PBFI (AM forms) and an equivalent concentration of Pluronic 20% in DMSO at room temperature (18–25 °C) for 20–30 min. After washout, cells were allowed 30 min to 1 h before they were added to the bath of the setup and left to sediment.

The bath was located at the stage of an inverted epi-fluorescence microscope (Axiovert 100, Zeiss) equipped with a Fluar ×40/1.30 NA oil immersion objective. Excitatory light was provided by a xenon arc lamp light source. The dyes were excited alternatively at 340 and 380 nm wavelengths (Omega Optical, Inc., VT) by means of an optical filter changer (Lambda 10-2, Sutter Instruments, CA). Emitted light was filtered at 510 nm band-pass and acquired by an intensified CCD camera (Extended ISIS, Photonic Science Ltd., UK). Results are presented as the relative change ($-\Delta F/F_o$) of the F_{340}/F_{380} signal. Significance was calculated with Student's *t*-test for paired observations.

2.5. Chemicals

BEA is poorly soluble in water, therefore a stock solution with Tween 80/MeOH = 1:2 was prepared for compound stability. This solution was further diluted in the bathing solution at the final concentration. Fluorescent dyes and Pluronic F-127 were procured from Molecular Probes (Leiden, The Netherlands). All other chemicals were purchased from Sigma (Sigma-Aldrich Chemie, Steinheim, Germany).

3. Results

3.1. Control experiments

All patches were initially superfused with bathing solutions in the absence of BEA during a control period of 10 min. In this condition, clamping at different holding potentials (E_h) (− 80 to + 80 mV for ventricular myocytes, − 200 to + 100 mV for synthetic membranes) did not reveal any current.

3.2. Channel-forming activity of BEA

Channel-forming activity of BEA was detected both in inside–out patches of ventricular myocytes and in synthetic membranes bathed in the SAS. Ten to fifteen minutes after BEA addition to the superfusate, application of various E_h revealed a complex, multilevel channel activity. Discrete current transitions, typical for channel-forming substances, from the closed (C) to several conducting (O) states were apparent within several minutes after wash-in initiation (Fig. 1A).

Fig. 1B presents examples of current records of a single BEA channel in steady state when an FTL-free patch was clamped at successively increasing positive or negative potentials. Patches were held at the potentials indicated for typically 2–5 min. At negative potential differences, clear transitions between the closed state (C) and a main open conductance state (O_2) were observed. At least one additional conductance level (O_1) was present (see current record at − 100 mV, but also Fig. 1A and C). At large positive potentials (above + 50 mV), the channel activity was characterized by a pronounced flickering behavior with high-frequency oscillations and usually without any clear constant current level. The same phenomenon was observed in myocytes.

Incorporation of new channels continued with time, resulting in the presence of multiple channels (Fig. 1C). As a result, openings fired from a new level of higher conductance with time, while a return to the initial level was rarely observed. States were relatively more distinguishable in the FTL system because of the lower frequency of transitions. Higher BEA concentrations produced similar effects with a faster onset of action. Washout of the substance was not effective, indicating a more permanent incorporation in the cell's membrane.

It was concluded that BEA is a potent channel-forming substance that incorporates spontaneously in the membrane of ventricular myocytes and in synthetic membranes.

3.3. Conductance states

Potassium ions gave rise to better defined single channel events in comparison to the other conducting cations tested. In myocytes, two main permeating events, O_1 and O_2, were distinguishable at the very beginning of BEA wash-in

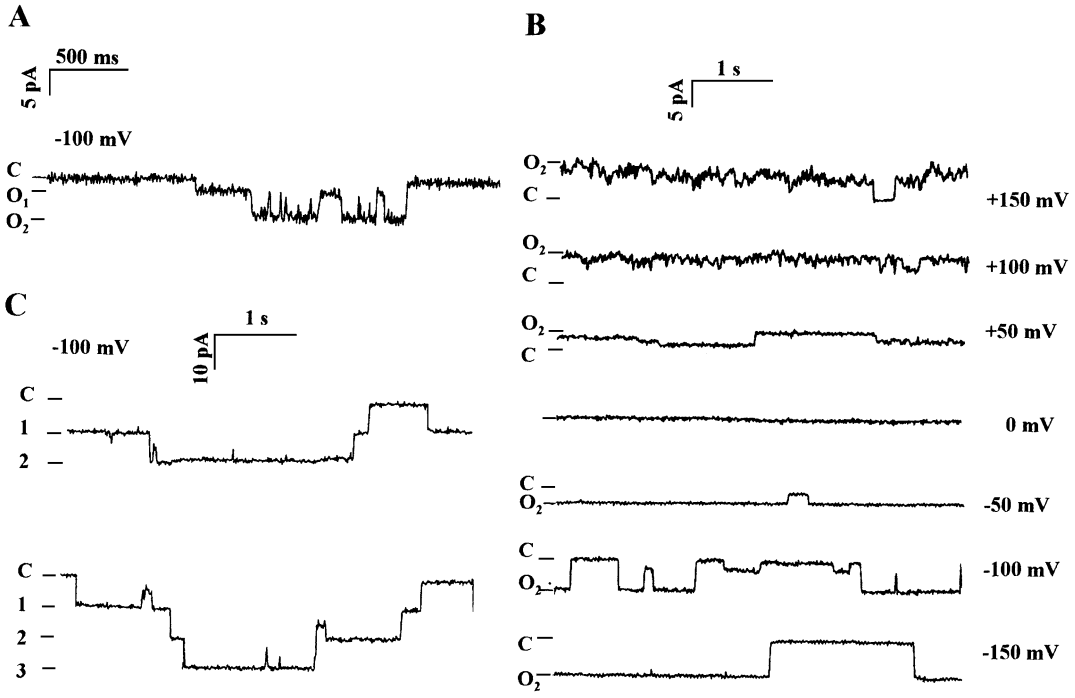

Fig. 1. Current records of BEA channels after spontaneous incorporation in synthetic membranes symmetrically bathed in SAS. C represents the closed level in all cases. (A) Current record recorded during incorporation of a single BEA channel. It illustrates the first events observed about 1 min after adding BEA at a final concentration of 10 μM in the bathing solution. Note the presence of two conducting states O_1 and O_2. (B) Current records of a single BEA channel clamped at successive increasing and decreasing potential differences. (C) Current records of a patch believed to contain three BEA channels (designated 1, 2, 3).

($n=10$, Fig. 2A). An additional third level, O_3, was also observed. The appearance of complete channel openings and closures to and from the three different conductance levels in the same patch suggests the existence of a channel with substates. In one of the single channel patches, the probabilities of occurrence of the O_1 and O_2 events were calculated. Their product was not equal to the probability of simultaneous occurrence of O_1 and O_2 in this patch, thus failing to support their independence. Superposition of O_3 with either of the two events was not observed. In light of the above, the O_1 and O_2 levels are likely substates, while the O_3 level may correspond to the full conductance of the channel.

Incorporation of the channel in synthetic membranes provided further evidence for the presence of several conductance states. Besides the main open (O_2) and the closed (C) state, at least one additional conducting state (O_1) was observed (Fig. 1, at -100 mV). In all patches investigated in detail ($n=8$) both conductance levels were present. The smaller conductance level was only observed in the presence of the larger conductance state and never alone. In this synthetic membrane system, only one channel-forming entity was present, hence different conductance states have to be substates of the same channel-forming entity by definition. It cannot be excluded that other substates are present, but they were not consistently observed in this system.

At least one substate O_1 (Fig. 3, traces c and e) and a higher conductance state O_2 (Fig. 3, traces a, b and d) were detected for currents carried by Na^+ ions in myocytes ($n=10$). Although only two conducting states were clearly resolved, the possibility of the existence of more conducting states is not excluded.

3.4. Permeating cations and selectivity of the BEA channel

The experimental E_{rev} for potassium ($n=3$) and sodium ($n=3$) in myocytes and for potassium in synthetic membranes ($n=7$) were comparable to the theoretical values for the ionic equilibrium potential calculated according to the

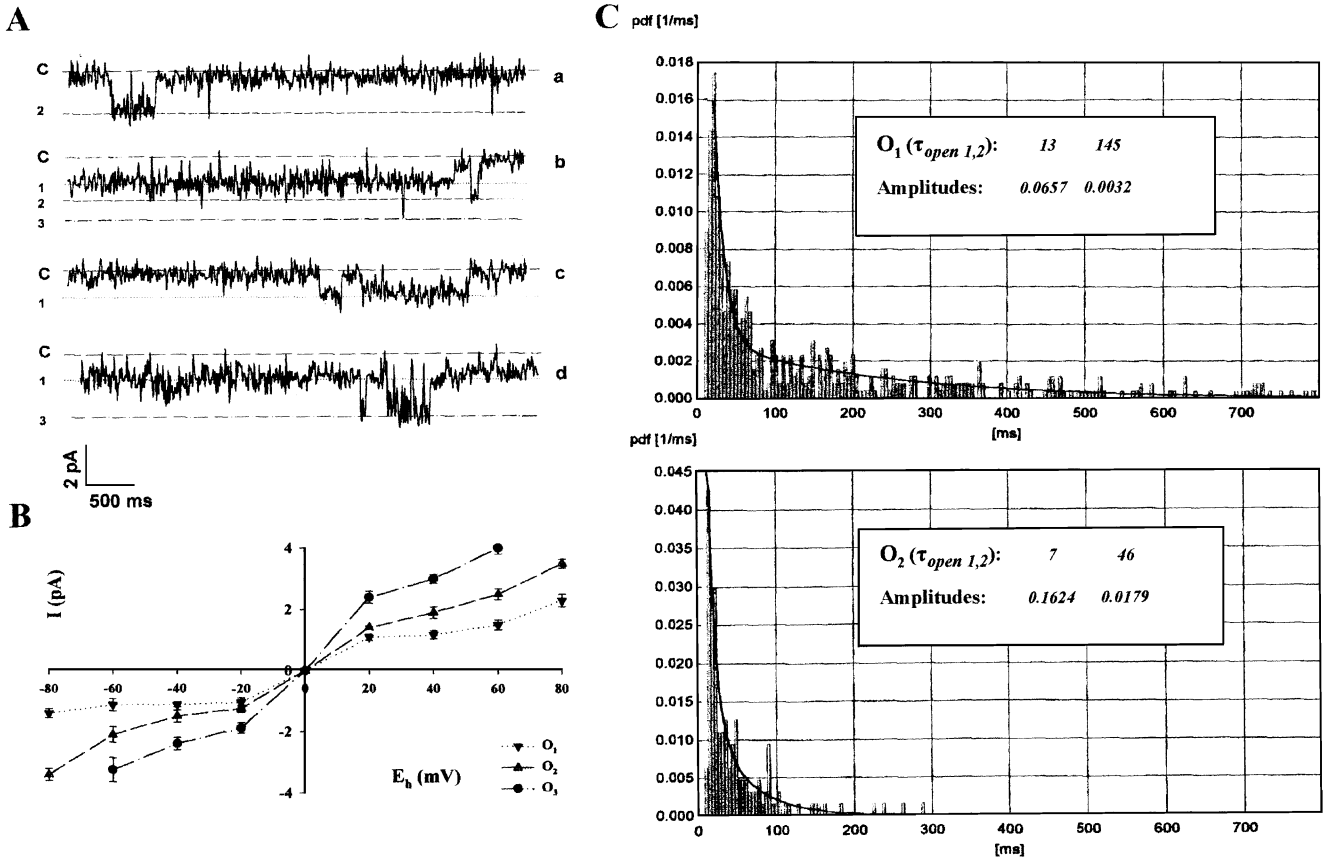

Fig. 2. Conductance and kinetics of BEA-induced K^+ currents. (A) Original traces of BEA-induced K^+ currents in an inside–out patch of a ventricular myocyte. The patch was clamped at a holding potential of -40 mV. C denotes the closed level. Openings to O_1 (dotted line 1) are seen in traces b, c and d; openings to O_2 (dashed line 2) are seen in traces a and b; O_3 is visible in traces b and d (dash-dotted line 3). The O_3 may appear as a subsequent superposition of O_1 and O_2 (trace b) or as direct complete transitions between levels C and 3 (trace d). (B) Current to voltage relationships for all three states observed in BEA-induced K^+ currents. *I-V* behavior and rectification upon higher potentials is similar for all. Conductance was calculated from -20 to $+20$ mV. (C) Open times histograms for the two substates O_1 (upper panel) and O_2 (lower panel) observed in BEA-induced K^+ currents. Probability density functions are fitted with two exponentials. Insets indicate time constants in milliseconds and their respective amplitudes. Note the longer duration exhibited by channel openings to substate O_1. Events that could be fitted by the larger exponential function are in both cases less frequently encountered.

Fig. 3. Original traces of BEA-induced Na^+ inward currents in an inside–out patch of a ventricular myocyte. The patch was clamped at a holding potential of −40 mV. C denotes the closed level. Openings to O_1 are visible in traces c and e. Openings to O_2 may be seen in traces a, b and d.

Nernst equation. Indeed, when the applied holding potential was held at E_K or E_{Na}, no net ionic flux was observed. This was a clear indication of the channel's cationic selectivity. The permeability ratio for the two cations was found $P_K/P_{Na} = 1.4$ ($n = 3$), indicating a higher selectivity for the K^+ ions.

Substitution of aspartate for sulfate and chloride in the K^+ and Na^+ bathing solutions in equal cation molarity did not affect the experimental E_{rev} ($n = 20$). This demonstrated that, like aspartate, neither sulfate nor chloride anions could gain access through the pore despite their variable dimensions and charge.

Electrical activity was also induced in myocytes after BEA wash-in with Li^+ ($n = 3$), Ca^{2+} ($n = 7$) and Mg^{2+} ($n = 7$) as charge carriers, indicating that BEA can also conduct divalent cations in mammalian cell membranes, albeit with different selectivity (in one experiment, a permeability ratio of $P_K/P_{Ca} \sim 10$ was observed) and different kinetics (see below).

3.5. Conductance

The *I-V* plots for all three conducting states of the potassium current (Fig. 2B) presented a symmetrical behavior upon hyper- and depolarization, rectifying at potentials higher than −40 and +40 mV. Single channel conductance was therefore estimated in the linear range of −20 to +20 mV and was calculated for O_1 at 51 ± 2.6 pS, for O_2 at 76.4 ± 1.2 pS and for O_3 at 107 ± 6.3 pS ($n = 10$). The similar *I-V* shape for all states could suggest a similarity in their respective conducting configurations. Mean conductance values for currents carried by Na^+ ions were 47.5 ± 4.5 pS (Fig. 3, traces c and e) for O_1 and 62.7 ± 2.2 pS (Fig. 3, traces a, b and d) for O_2 ($n = 10$).

In synthetic membranes, bathing in the SAS, the mean conductance values of the BEA channel were (in pS) 36.3 ± 6.2 and 96.8 ± 11.7 ($n = 8$) for the O_1 and O_2 conducting states, respectively. The conductance was estimated between −50 and +50 mV, because in this system, rectification at more extreme voltages (both positive and negative) was also observed.

3.6. Kinetics

Continuous incorporation of BEA channels in the patch complicated the kinetic analysis. For that reason, analysis was performed in a short period of time immediately following BEA wash-in in patches containing one channel.

Probability density functions for open times of the BEA channel conducting K^+ and Na^+ cations ($E_h = -60$ to +60 mV) were best fitted with two exponentials (Fig. 2C). The kinetics of the openings at those potentials were not significantly affected by voltage. Open times τ and P_o of the observed events are presented in Table 1. Open times for the conductance state O_3 were not calculated because of the inadequacy of the number of observations to produce a reliable statistical analysis. The time constants (in ms) for the closed states were 8 ± 2 and 175 ± 20 (O_1 state), and 12 ± 4 and 628 ± 245 (O_2 state) for the first and second exponentials, respectively ($n = 10$).

In synthetic membranes, residing times in the respective states were best fitted with two exponentials. Between +50 and −150 mV the kinetics of the closed and the main open state were not significantly affected by voltage. Time constants (in ms) and P_o for the O_2 state are given in Table 1. Transitions to O_1 were too rare for reliable analysis. For the closed state the time constants (in ms) were 36.7 ± 26.3 and 746 ± 285 for the first and the second exponential, respectively ($n = 3$). Residing times of the pore in the respective conducting states in artificial biological membranes were longer as compared to the same pore in membranes of ventricular myocytes (Table 1).

Table 1
Open times τ (ms) and P_o for the BEA conductance states observed for K^+ and Na^+ in myocytes and liposomes

	$K^+_{myocyte}$ [a]			$Na^+_{myocyte}$ [a]		K^+_{FTL} [b]	
	O_1	O_2	O_3	O_1	O_2	O_1	O_2
τ_1	13.2 ± 1.2	7.5 ± 1.7	–	9.3 ± 3	5.8 ± 0.8	–	106.5 ± 10.9
τ_2	145 ± 16.5	46 ± 5.4	–	159 ± 22	67 ± 16	–	4397 ± 1797
P_o	0.58 ± 0.12	0.027 ± 0.07	$< 10^{-3}$	0.52 ± 0.18	0.025 ± 0.01	–	0.51 ± 0.30

[a] $n = 10$.
[b] $n = 3$.

Ca^{2+} ions (open times: $\tau_1 = 1.34 \pm 0.3$ ms, $\tau_2 = 15-150$ ms; $n = 3$) and Mg^{2+} ions (open times: $\tau_1 = 1.8 \pm 0.2$ ms, $\tau_2 = 30 \pm 8$ ms; $n = 3$) were conducted with faster channel kinetics. Openings occurred usually in bursts of fast flickerings, which alternated with periods of electrical inactivity. Low conductance–slow kinetics events as described for the monovalent cations were not observed.

It was concluded that the kinetic of the BEA channel was not only influenced by the type of membrane the channel was incorporated in, but also by the conducting cation.

3.7. Blocking of the BEA channel

Block by La^{3+} (10 μM up to 1 mM) was tested in synthetic membranes (Fig. 4, $E_h = -100$ mV, $n = 10$) and myocytes ($E_h = -60$ to $+60$ mV, $n = 3$). In all trials, a reduction of the apparent current level was observed, which depended on the administered blocker concentration. Even at the highest concentration applied the current was not completely abolished. The block was only partially reversible in the SAS, but the current was completely restored after washout with EDTA (10 mM) for 15 min.

A relative reduction of 40% (myocytes, $E_h = -60$ to $+60$ mV, $n = 5$) of the macroscopic current could be observed upon increasing Ca^{2+} concentration up to 5 mM in the bathing solution containing monovalent cations, suggesting that in the presence of monovalent cations, divalent may exert a blocking effect.

3.8. Effects on the physiological ion concentrations of myocytes

FURA 2AM loaded myocytes subjected to 10 μM BEA began to spontaneously contract within 10–15 min. Prominent effects were a $[Ca^{2+}]_i$ increase and an ensuing Ca^{2+} overload accompanied with loss of rod shape.

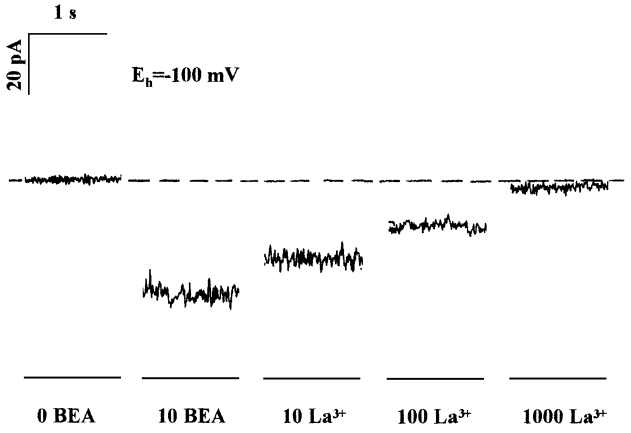

Fig. 4. La^{3+} block of the BEA channel incorporated in synthetic membranes (concentrations all given in μM). The patch is bathed in SAS solution. At left, a control current trace is illustrated in the absence of BEA. The second trace from the left is the steady state current level after wash-in of 10 μM BEA. Subsequent current traces illustrate the effect of increasing concentrations of La^{3+} (10, 100 and 1000 μM) in the presence of 10 μM BEA. The apparent current level decreased but was not completely reduced to the control level.

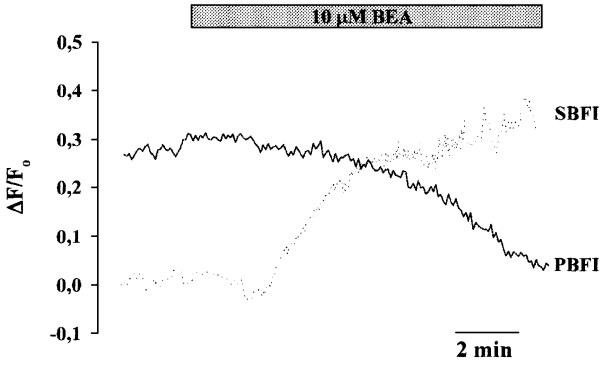

Fig. 5. Effects of BEA on the $[K^+]_i$ and $[Na^+]_i$ of ventricular myocytes. Relative F_{340}/F_{380} fluorescence intensities from averaged responses are depicted against time. Reduction in the fluorescence intensity of PBFI-loaded cells indicates a reduction of $[K^+]_i$ ($n = 5$, $P < 0.005$). Increase in the SBFI fluorescence intensity is associated with a $[Na^+]_i$ increase ($n = 5$, $P < 0.001$).

Ratiometric experiments on cardiomyocytes loaded with SBFI showed an increase in $[Na^+]_i$ a few minutes after application of 10 μM BEA in the bath ($n = 5$, Fig. 5). Contrary to that, cells loaded with PBFI and treated by BEA showed a gradual, persistent decrease in fluorescence intensity with a faster onset. Extracellular application of potassium channel blockers (Cs^+ and TEA), did not abolish the instant slow decline in fluorescence intensity, which probably reflects the slow leak of K^+ through the BEA pores out of the cell membrane ($n = 5$).

4. Discussion

4.1. BEA is a channel-forming substance

The above results provide evidence that BEA readily incorporates in mammalian cells and synthetic membranes, in which it forms cation-selective channels. Despite its structural analogy to the cyclic dodecadepsipeptide valinomycin, a K^+-selective neutral ion-carrier, patch clamp studies reveal that BEA manifests common traits of physiological ion channel behavior such as unitary transitions in conductance levels characteristic for channels, selectivity, rectification, conductances in the pS range, substates and block. These strongly suggest that BEA is a potential channel-forming ionophore. Being able to build pores is not excluding a concomitant role as a carrier as proposed before [12].

In a recent report, BEA was described as a specific inhibitor of the L-type Ca^{2+} current in NG108-15 cells [11]. The full effect was already measured at 2 min after application of 10 μM BEA. Under our experimental conditions, however, the BEA-induced single channel currents were first observed in FTLs beginning from 1 to 2 min at a concentration of 10 μM BEA gradually developing over a period of about 10–15 min. Furthermore, the effect was

minimally reversible, if at all, in contrast to the completely reversible washout of the BEA-induced block of the Ca^{2+} current. In addition, BEA has been found to complex divalent cations [12,13].

4.2. A proposed model for the BEA pore

In accordance with the sandwich complexes proposed by Ivanov et al. [16], a similar energetically favored configuration may be assumed that consists of vertically stacked BEA molecules. The complex would span the membrane and provide access to ions from either end of the pore, enabling net diffusion down their electrochemical gradient at both directions. This conformation would allow the symmetry depicted in the *I-V* plots and the sort of electrostatic interaction that prevailed in our experiments, making the pore selective to cations. Much like the antibiotic–cation complexes [15], an electrostatic interaction of the permeating cation with the O-ligands of neighboring BEA molecules during conduction is apparent. As evidence was found that the kinetics of the channel were influenced by the conducted cation, it is likely that the permeant ion plays a significant role in the stabilization of the conducting conformation.

4.3. Conductance and substates of the pore

The appearance of different non-integral multiple conductance states could indicate a barrel-stave model conformation. However, alamethicin-type multistate pores lose their ionic selectivity and show a typical pattern of consecutive increasing conductance levels because of monomer addition. In our experiments, we found no evidence that higher conductance levels show an altered selectivity for cations versus anions. Furthermore, a barrel-stave like model would leave three O atoms exposed to the lipid membrane. The conductance levels observed seem to conform to the reported 3/2 rule for channels with multilevels of conductance, which is mathematically incompatible with the barrel-stave model [21]. The principal state conductances were not significantly affected by variable membrane properties; therefore the BEA channel is more likely a pore of fixed structure rather like the gramicidin type. Indeed, the BEA pore presents similarities with the gramicidin dimer like anionic impermeability, cation selectivity in the order of $K^+ > Na^+ > Li^+$ [22], block by divalent cations and subconductance states [23].

4.4. Selectivity of the pore

It is believed that the molecular mechanisms governing selectivity in complexing cations are similar to those defining the selectivity of the pore. Consistent with a narrow pore configuration, the channel's functional site is located in the molecule's inner cavity lined by polar peptide groups, which provide the hydrophilic environment required for ionic conductance. The carbonyl oxygen atoms increase the electronegative character of the pore, explaining the cation selectivity that the E_{rev} and anionic substitution experiments demonstrated. The cage of BEA lined with several kinds of atoms has a radius of 2.7–3 Å; the oxygen-ligand array radius can be approximated to 2.2 Å, based on Hiv- and Phe-oxygen distances of free and complexed BEA provided by X-ray crystallographic data [24]. The O-ligands are flexible to accommodate ions of different size. These dimensions are comparable to the gramicidin A channel pore (radius ~ 2 Å, [25]). That kind of diameter could easily accommodate a dehydrated K^+ ($r = 1.33$ Å) and account for the higher K^+ selectivity.

4.5. Kinetics of the pore

BEA channel kinetics in the order of milliseconds indicate the transient nature of each conducting conformation. This could be partly attributed to the lack of stability in monomer association, as compared to gramicidin dimers, whose longer lifetimes are believed to reflect the stability offered by the hydrogen bonds [26]. Differences in BEA pore kinetics after incorporation in FTLs (slower kinetics) and myocytes (faster kinetics) and the occasional flickering behavior may be explained in terms of channel stability and lifetimes being directly related to membrane properties [27,28]. Different membrane composition, thickness and tension may affect the channel formation and dissociation rates [28,29], and the flickering frequency, as in the SS dimers of gramicidin, where increased flickering reflects the membrane deformation of thicker bilayers [30].

4.6. Physiologic effects of the BEA pore

Fluorescence measurements clearly show that BEA's channel-forming activity in physiological membranes as proven by the patch clamp has a direct effect on the intracellular ion concentration of mammalian cells. BEA's channel-forming activity at the cellular level increases membrane permeability towards monovalent cations and tends to collapse the cationic gradients. Net cationic influx is consistent with the membrane resting potential depolarization observed in papillary muscles and BEA's ionophoric activity may thus account for the previously reported results on cardiac toxicity [10]. The $[Ca^{2+}]_i$ increase measured in ventricular myocytes agrees with the reported $[Ca^{2+}]_i$ rise and apoptosis following BEA application in tumor cell lines [7]. Disturbance of the normal physiological concentrations of important monovalent and divalent cations could account, at least in part, for the non-specific toxicity of BEA to mammalian cells, insects and microbes.

Acknowledgements

K. Kouri was partly supported by the Austrian Science Foundation (FWF) with the project P14507-PHA.

References

[1] R.K. Hamill, C.E. Higgens, H.E. Boaz, M. Gorman, Tetrahedron Lett. 49 (1969) 4255–4258.
[2] S. Gupta, S.B. Krasnoff, N.L. Underwood, J.A.A. Renwick, Mycopathologia 115 (1991) 185–189.
[3] A. Logrieco, A. Moretti, G. Castella, M. Kostecki, P. Golinski, A. Ritieni, J. Chelkowski, Appl. Environ. Microbiol. 64 (1998) 3084–3088.
[4] D.B. Prelusky, B.A. Rotter, R.G. Rotter, Mycotoxins in grain compounds other than aflatoxin, in: J.D. Miller, H.L. Trenholm (Eds.), Toxicology of Mycotoxins, Eagan Press, St. Paul, MN, USA, 1994, pp. 359–403.
[5] A. Vey, J.M. Quiot, C. Vago, Compt. Rend. (D) 276 (1973) 2489–2492.
[6] J.F. Grove, M. Pople, Mycopathologia 70 (1980) 103–105.
[7] D.M. Ojcius, A. Zychlinsky, L.M. Zheng, J.D. Young, Exp. Cell Res. 197 (1991) 43–49.
[8] H. Tomoda, X.H. Huang, J. Cao, H. Nishida, R. Nagao, S. Okuda, H. Tanaka, S. Omura, H. Arai, K. Inoue, J. Antibiot. (Tokyo) 45 (1992) 1626–1632.
[9] S. Nakajyo, K. Matsuoka, T. Kitayama, Y. Yamamura, K. Shimizu, M. Kimura, N. Urakawa, Jpn. J. Pharmacol. 45 (1987) 317–325.
[10] R. Lemmens-Gruber, R. Rachoy, E. Steininger, K. Kouri, P. Saleh, R. Krska, R. Josephs, M. Lemmens, Mycopathologia 149 (2000) 5–12.
[11] S.N. Wu, H. Chen, Y.C. Liu, H.T. Chiang, Chem. Res. Toxicol. 15 (2002) 854–860.
[12] R.C. Prince, A.R. Crofts, L.K. Steinrauf, Biochem. Biophys. Res. Commun. 59 (1974) 697–703.
[13] R.W. Roeske, I. Sherwin, T.E. King, L.K. Steinrauf, Biochem. Biophys. Res. Commun. 57 (1974) 554–561.
[14] R. Benz, J. Membr. Biol. 43 (1978) 367–394.
[15] Y.A. Ovchinnikov, V.T. Ivanov, A.V. Evstratov, I.I. Mikhaleva, V.F. Bystrov, S.L. Portnova, T.A. Balashova, E.N. Meshcheryakova, V.M. Tulchinsky, Int. J. Pept. Protein Res. 6 (1974) 465–498.
[16] V.T. Ivanov, A.V. Evstratov, L.V. Sumskaya, E.I. Melnik, T.S. Chumburidze, S.L. Portnova, T.A. Balashova, Y.A. Ovchinnikov, FEBS Lett. 36 (1973) 65–71.
[17] K. Kouri, C. Studenik, R. Lemmens-Gruber, Biophys. J. 82 (2002) 554a (abstr.).
[18] R. Mitra, M. Morad, Am. J. Physiol. 249 (1985) H1056–H1060.
[19] O.P. Hamill, A. Marty, E. Neher, B. Sakmann, F.J. Sigworth, Pflugers Arch. 391 (1981) 85–100.
[20] M. Lemmens, K. Verheyden, P. Van Veldhoven, J. Vereecke, G.P. Mannaerts, E. Carmeliet, Biochim. Biophys. Acta 984 (1989) 351–359.
[21] J.R. Pollard, N. Arispe, E. Rojas, H.B. Pollard, Biophys. J. 67 (1994) 647–655.
[22] V.B. Myers, D.A. Haydon, Biochim. Biophys. Acta 274 (1972) 313–322.
[23] D. Busath, G. Szabo, Biophys. J. 53 (1988) 689–695.
[24] J.A. Hamilton, L.K. Steinrauf, B. Braden, Biochem. Biophys. Res. Commun. 64 (1975) 151–156.
[25] B.A. Wallace, Annu. Rev. Biophys. Biophys. Chem. 19 (1990) 127–157.
[26] C.M. Venkatachalam, D.W. Urry, J. Comput. Chem. 4 (1983) 461–469.
[27] S.B. Hladky, D.A. Haydon, Biochim. Biophys. Acta 274 (1972) 294–312.
[28] J.R. Elliott, D. Needham, J.P. Dilger, D.A. Haydon, Biochim. Biophys. Acta 735 (1983) 95–103.
[29] M. Goulian, O.N. Mesquita, D.K. Fygenson, C. Nielsen, O.S. Andersen, A. Libchaber, Biophys. J. 74 (1998) 328–337.
[30] K.M. Armstrong, S. Cukierman, Biophys. J. 82 (2002) 1329–1337.